Other models

• Model with human ovary

Terada, Y., Y. Terunuma-Sato, T. Kakoi-Yoshimoto, H. Hasegawa, T. Ugajin, Y. Koyanagi, M. Ito, T. Murakami, H. Sasano, N. Yaegashi, and K. Okamura. 2008. Development of human Graafian follicles following transplantation of human ovarian tissue into NOD/SCID/gammac null mice. *Am J Reprod Immunol* 60:534-540.

Transplantation of human ovarian cortex into host mice may permit various kinds of challenges in reproductive medicine. A novel immunodeficient mouse strain (NOD/SCID/gammac null: NOG) has been developed as a host for transplantation of human tissue. Human ovarian cortex was transplanted into various sites of NOG mice and human follicular development was examined by immunohistochemistry. Transplantation of human ovarian tissue into NOG mice resulted in approximately similar tissue survival and follicle growth as did transplantation into non-obese diabetic-severe combined immunodeficient mice. The human Graafian follicle from NOG mouse expressed the same steroidogenic enzymes as observed in human Graafian follicles, which developed in the human body. The NOG mice's ovarian bursa was better placed for transplantation than the back skin or kidney capsule. These results represent the successful generation and biological confirmation of the human Graafian follicles from the human ovarian cortex in the NOG mice.

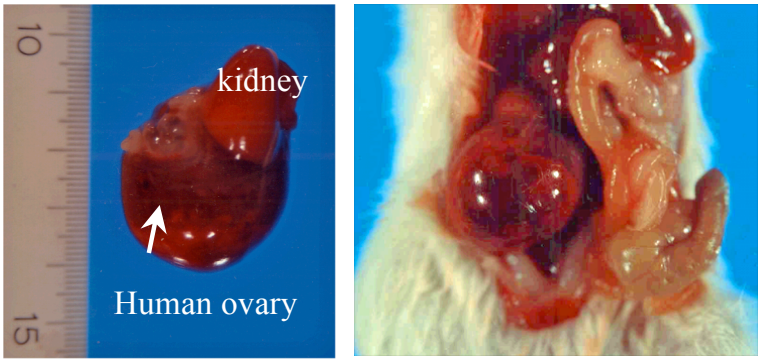

Figure 1. Macroscopic view of a human Graafian follicle (arrow) after transplantation of human ovarian cortex into the ovarian bursa of a NOG mouse.
Host mice were stimulated by daily intraperitoneal injection of human menopausal gonadotropin for 14 days, 10 weeks after transplantation. Scale bar = 1 cm.

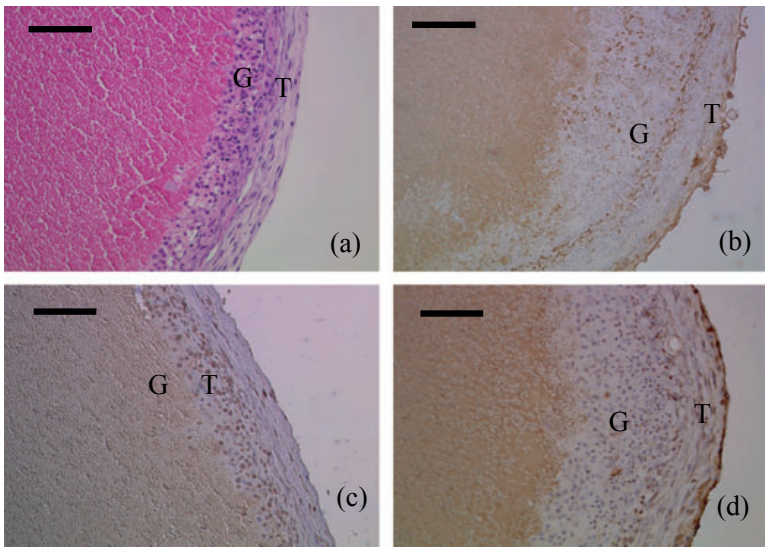

Figure 2. Characterization of a human Graafian follicle that developed in the ovarian bursa of a NOG mouse.
(a) Hematoxylin and eosin staining showing the theca and granulosa cell layers. (b) Antibody staining for the steroidogenic enzyme P450 scc is localized to the cytoplasm of theca cells. (c) Immunohistochemistry for AD4-BP showing expression in the nuclei of both theca and granulosa cell layers. (d) ER antibody staining was detected in the theca cell layer. T, theca cells; G, granulosa cells. Scale bar = 100 µm.

Other models

• Model with human endometrium

Matsuura-Sawada, R., T. Murakami, Y. Ozawa, H. Nabeshima, J. Akahira, Y. Sato, Y. Koyanagi, M. Ito, Y. Terada, and K. Okamura. 2005. Reproduction of menstrual changes in transplanted human endometrial tissue in immunodeficient mice. *Hum Reprod* 20:1477-1484.

Cultures of human endometrial tissue are useful for analysing the mechanisms underlying the menstrual cycle. However, long-term culture of endometrial tissue is difficult in vitro. Xenotransplantation of normal human endometrial tissue into immunodeficient mice could allow prolonged survival of the transplanted tissues. Proliferative-phase endometrial tissue samples from three women were transplanted into the subcutaneous space of ovariectomized, immunodeficient, non-obese diabetic (NOD)/severe combined immunodeficiency (SCID)/gammaC(null) (NOG) mice. The mice were treated with 17beta-estradiol (E2) for the first 14 days after transplantation, followed by E2 plus progesterone for the next 14 days. The transplants were investigated morphologically and immunohistochemically at various times after implantation. The transplanted tissues contained large numbers of small glands, pseudostratification of the nuclei and dense stroma after treatment with E2 alone. After treatment with E2 plus progesterone, subnuclear vacuolation, luminal secretion and decidualization of the stroma were observed. When the hormone treatment ceased, tissue destruction occurred and the transplants returned to the proliferative phase. Lymphocytes were identified immunohistochemically: the numbers of CD56-positive and CD16-negative cells increased significantly in the stroma during the late secretory phase (day 28). Human endometrial tissue transplanted into NOG mice showed similar histological changes to eutopic endometrial tissue during treatment with sex steroid hormones for 1 month. Moreover, lymphocytes were produced in the transplanted human endometrial tissue. This system represents a new experimental model of the human endometrium in vivo.

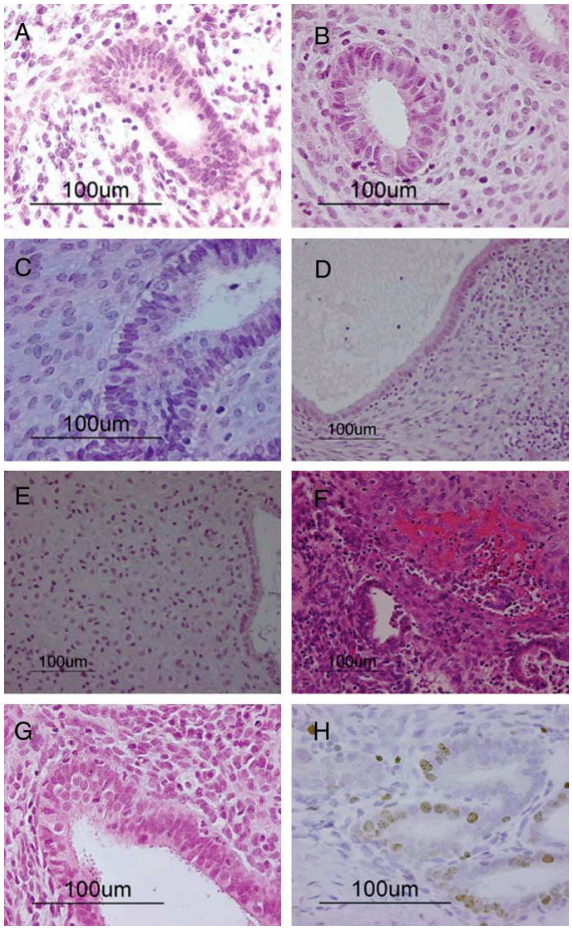

Figure 1. Histological sections stained with haematoxylin and eosin (A–G) and the immunohistochemical stain Ki-67 (H). (A) Pretransplantation endometrial tissue: the proliferative phase. The glands are small straight and narrow, with columnar glandular cells and prominent pseudostratification of the nuclei. The stromal cells are dense (magnification ×400). (B) Endometrial tissue 14 days after transplantation: E_2 has been administered for 14 days. The glands are small and narrow, with tall columnar cells. Evidence of pseudostratification of the nuclei is present. The stromal cells are dense (magnification ×400). (C) Endometrial tissue 16 days after transplantation: E_2 has been administered for 14 days, followed by E_2 plus progesterone for 2 days. The glands still show pseudostratified structures but they have begun to enlarge, and subnuclear vacuolation of the glandular cells is visible. The stromal cells remain dense (magnification ×400). (D) Endometrial tissue 21 days after transplantation: E_2 has been administered for 14 days, followed by E_2 plus progesterone for 7 days. The glands are significantly dilated, the glandular cells are cuboidal and the pseudostratification of the nuclei has disappeared. Stromal decidualization is beginning. Many lymphocytes are present throughout the stroma and are aggregating around the glands (magnification ×200). (E) Endometrial tissue 28 days after transplantation: E_2 has been administered for 14 days, followed by E_2 plus progesterone for 14 days. The glandular cells are cuboidal. Evidence of stromal decidualization is clearly seen and lymphocytes are present in the stroma (magnification ×200). (F) Endometrial tissue 31 days after transplantation: E_2 had been administered for 14 days, followed by E_2 plus progesterone for 14 days, and then no hormones for the remaining 3 days. The glands and endometrial stroma have collapsed during the evolution of the transplant. There is prominent bleeding in the stroma (magnification ×200). (G) Endometrial tissue 35 days after transplantation: E_2 had been administered for 14 days, followed by E_2 plus progesterone for 14 days, and then no hormones for the remaining 7 days. The glands are small and narrow with tall columnar cells. Evidence of pseudostratification of the nuclei is present. The stromal cells are dense (magnification ×400). (H) Endometrial tissue 35 days after transplantation: a number of nuclei have been immunohistochemically stained with Ki-67, showing proliferation of glandular and stromal cells (magnification ×400).

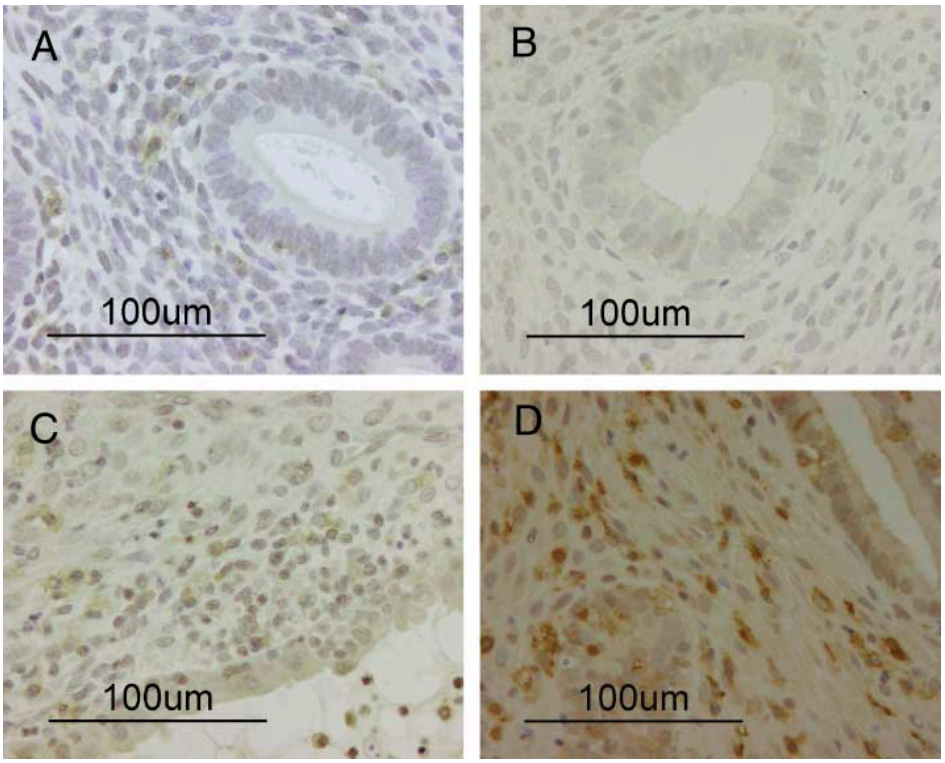

Figure 2. Immunohistochemical staining of human CD56.
(A) Pretransplantation endometrial tissue: human CD56-positive cells are present in small numbers (magnification ×400). (B) Day 14 after transplantation: human CD56-positive cells have completely disappeared from the stroma (magnification ×400). (C) Day 21 after transplantation: human CD56-positive cells are present in small numbers (magnification×400). (D) Day 28 after transplantation: human CD56-positive cells have significantly increased in number in the stroma (magnification ×400).

Other models

• Efficacy test model for thrombopoietic drugs

Nakamura, T., Y. Miyakawa, A. Miyamura, A. Yamane, H. Suzuki, M. Ito, Y. Ohnishi, N. Ishiwata, Y. Ikeda, and N. Tsuruzoe. 2006. A novel nonpeptidyl human c-Mpl activator stimulates human megakaryopoiesis and thrombopoiesis. *Blood* 107:4300-4307.

NIP-004 is a novel synthetic compound developed to display human thrombopoietin (TPO) receptor (c-Mpl) agonist activity. NIP-004 displays species specificity, stimulating proliferation or differentiation of human c-Mpl–expressing cells such as UT-7/TPO and human CD34(+) cells but not murine c-Mpl–expressing cells or cynomolgus monkey cells. To test the mechanism of its action, we constructed mutant forms of c-Mpl; murine c-MplL490H displayed a response to NIP-004, where human c-MplH499L lost this response, indicating that histidine in the transmembrane domain of c-Mpl is essential for its activity. Because histidine is not present in the c-Mpl transmembrane domain of rats, hamsters, rhesus macaques, and cynomolgus monkeys, we examined the *in vivo* efficacy of NIP-004 using mice that received xenotransplants. In immunodeficient nonobese diabetic (NOD)/Shi-*scid,* IL-2Rgamma(null) (NOG) mice receiving transplants of umbilical cord blood–derived as CD34(+) cells, NIP-004 increased human megakaryoblasts, mature megakaryocytes, and circulating human platelets 6-fold, the latter being morphologically and functionally indistinguishable from normal human platelets. These observations indicate that NIP-004 is a novel human c-Mpl activator and induces human thrombopoiesis. (Blood. 2006;107: 4300-4307)

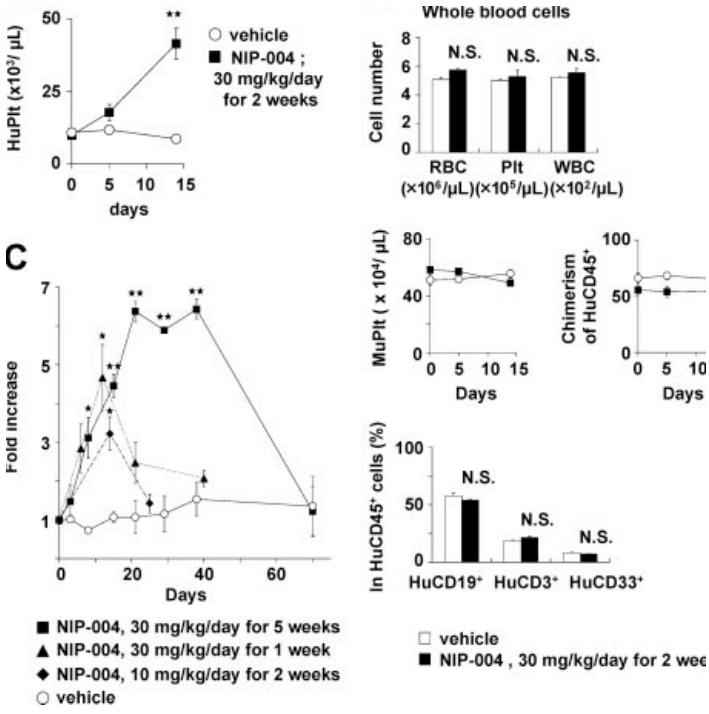

Figure 1. NIP-004–induced production of human platelets in NOG mice receiving xenotransplants.

(A) NIP-004 increased the number of circulating human platelets in NOG mice. (B) NIP-004 did not change the number of murine platelets or chimerism of HuCD45$^+$ cells. NIP-004 had no effect on the percentage of human B (CD19$^+$) cells, human T (CD3$^+$) cells, and human myeloid (CD33$^+$) cells in the peripheral HuCD45$^+$ cells. Data from panels A-B are expressed as the mean ± SEM (n = 3). (C) NIP-004 increased the number of circulating human platelets. The increase was calculated as the number of circulating human platelets at individual time points divided by the pretreatment value (day 0). Data are expressed as the mean ± SEM (n = 3 to 6) or mean ± SD (n = 2). *P < .05, **P < .01 between NIP-004 and vehicle at individual time points. N.S. indicates no significant differences compared with vehicle.

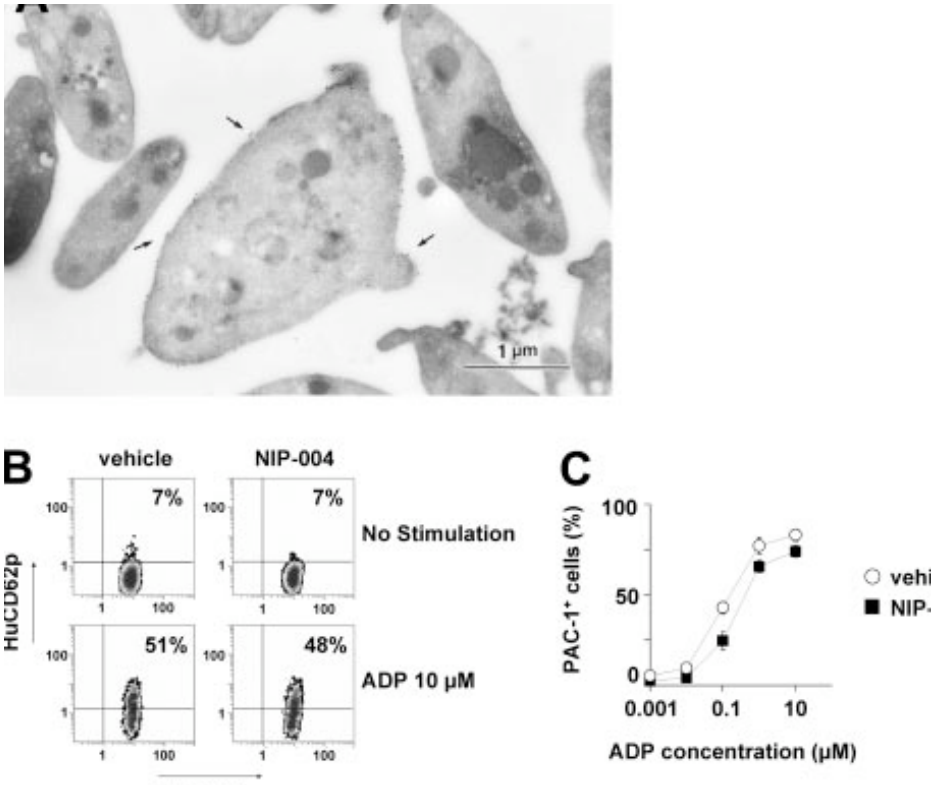

Figure 2. Morphologic and functional features of human platelets induced byNIP-004 in NOG mice.
(A) Immunoelectron microscopy using antibody against HuCD41a identified human platelets in PRP derived from NIP-004–treated mice. The surface of a platelet located in the center is labeled with gold particles (arrow), indicating that it is of human origin. Bar, 1 μm. (B) P selectin (HuCD62p) expression upon ADP stimulation in human platelets was similarly increased in both vehicle- and NIP-004–treated mice. (C) After stimulation with various concentrations of ADP, there was a similar dose-dependent escalation in the percentage of PAC-1–positive human platelets from vehicle- and NIP-004–treated NOG mice receiving xenotransplants. PAC-1 antibody specifically recognizes the activated form of GPIIbIIIa. Data are expressed as the mean ± SEM (n = 4).

Other models

• Safety test for human cell (ES, iPS, gene-manipulated cells) transplantation

K. Machida, H. Suemizu, K. Kawai, T. Ishikawa, R. Sawada, Y. Ohnishi, and T. Tsuchiya. 2009. Higher susceptibility of NOG mice to xenotransplanted tumors. *J Toxicol Sci* 34:123-127.

The purpose of tumorigenicity testing, as applied not only to cell substrates used for viral vaccine manufacture but also stem cells used for cell-based therapy, is to discriminate between cells that have the capacity to form tumors and cells that do not. Therefore, tumorigenicity testing is essential in assessing the safety of these biological materials. Recently developed NOD/Shi-*scid* IL2Rg^{null} (NOG) mice have been shown to be superior to NOD/Shi-*scid* (SCID) mice for xenotransplantation of both normal and cancerous cells. To select a suitable mouse strain as a xenogenic host for tumorigenicity testing, we compared the susceptibility of NOG (T, B, and NK cell-defective), SCID (T and B cell-defective), and the traditionally used nude (T cell-defective) mice to tumor formation from xenotransplanted HeLa S3 cells. When 10^4 HeLa S3 cells were subcutaneously inoculated into the flanks of these mice, the tumor incidence on day 22 was 10/10 (100%) in NOG, 2/10 (20%) in SCID, and 0/10 (0%) in nude mice. The subcutaneous tumors formed reproducibly and semiquantitatively in a dose-dependent manner. Unexpectedly, half of the NOG mice (5/10) that had been inoculated with a mere 10^1 HeLa S3 cells formed progressively growing subcutaneous tumors on day 78. We confirmed that the engrafted tumors originated from inoculated HeLa S3 cells by immunohistochemical staining with anti-HLA antibodies. These data suggest that NOG mice may be the best choice as a suitable strain for testing tumorigenicity.

Table 1. Comparative growth of HeLa S3 cells among BALB/cA *nu/nu*, NOD/Shi-*scid*, and NOG mice.

Cell dose	Sex	Number of mice with tumors (% engraftment)[a]		
(cells/head)		BALB/cA *nu/nu*	NOD/Shi-*scid*	NOG
$1x10^2$	Male	NT	0/5 (0%)	3/5 (60%)
	Female	NT	0/5 (0%)	3/5 (60%)
	Total	NT	0/10 (0%)	6/10 (60%) *
$1x10^3$	Male	0/5 (0%)	0/5 (0%)	3/5 (60%)
	Female	0/5 (0%)	0/5 (0%)	3/5 (60%)
	Total	0/10 (0%)	0/10 (0%)	6/10 (60%) #
$1x10^4$	Male	0/5 (0%)	2/5 (40%)	5/5 (100%) **
	Female	0/5 (0%)	0/5 (0%)	5/5 (100%) ##
	Total	0/10 (0%)	2/10 (20%)	10/10 (100%) ##
$1x10^5$	Male	5/5 (100%)	5/5 (100%)	NT
	Female	3/5 (60%)	4/5 (80%)	NT
	Total	8/10 (80%)	9/10 (90%)	NT

[a] Engraftment was evaluated 22 days after inoculation by 1 x 10^3, 10^4, and 10^5 cancer cells, and 43 days after inoculation by 1 x 10^2 cancer cells. Fisher's exact test was performed in statistical analysis. * $P < 0.05$ compared to the NOD/Shi-*scid* strain. ** $P < 0.01$ compared to the BALB/cA *nu/nu* strain. # $P < 0.05$ compared to the BALB/cA *nu/nu* and NOD/Shi-*scid* strain. ## $P < 0.01$ compared to the BALB/cA *nu/nu* and NOD/Shi-*scid* strain. NT: not tested.